2015

Antecedent moisture and temperature conditions modulate the response of ecosystem respiration to elevated CO_2 and warming

Edmund M. Ryan
Arizona State University

Kiona Ogle
Arizona State University

Tamara J. Zelikova
University of Wyoming, tzelikov@uwyo.edu

Dan R. Lecain
USDA-ARS, dan.lecain@ars.usda.gov

David G. Williams
University of Wyoming, dgw@uwyo.edu

See next page for additional authors

Authors

Edmund M. Ryan, Kiona Ogle, Tamara J. Zelikova, Dan R. Lecain, David G. Williams, Jack A. Morgan, and Elise Pendall

Global Change Biology

Global Change Biology (2015) **21**, 2588–2602, doi: 10.1111/gcb.12910

Antecedent moisture and temperature conditions modulate the response of ecosystem respiration to elevated CO_2 and warming

EDMUND M. RYAN[1], KIONA OGLE[1], TAMARA J. ZELIKOVA[2], DAN R. LECAIN[3], DAVID G. WILLIAMS[2], JACK A. MORGAN[3] and ELISE PENDALL[2,4]

[1]*School of Life Sciences, Arizona State University, Tempe, AZ, USA,* [2]*Department of Botany, University of Wyoming, Laramie, WY, USA,* [3]*USDA-ARS, Fort Collins, CO, USA,* [4]*Hawkesbury Institute for the Environment, University of Western Sydney, Penrith, NSW, Australia*

Abstract

Terrestrial plant and soil respiration, or ecosystem respiration (R_{eco}), represents a major CO_2 flux in the global carbon cycle. However, there is disagreement in how R_{eco} will respond to future global changes, such as elevated atmosphere CO_2 and warming. To address this, we synthesized six years (2007–2012) of R_{eco} data from the Prairie Heating And CO_2 Enrichment (PHACE) experiment. We applied a semi-mechanistic temperature–response model to simultaneously evaluate the response of R_{eco} to three treatment factors (elevated CO_2, warming, and soil water manipulation) and their interactions with antecedent soil conditions [e.g., past soil water content (SWC) and temperature (SoilT)] and aboveground factors (e.g., vapor pressure deficit, photosynthetically active radiation, vegetation greenness). The model fits the observed R_{eco} well (R^2 = 0.77). We applied the model to estimate annual (March–October) R_{eco}, which was stimulated under elevated CO_2 in most years, likely due to the indirect effect of elevated CO_2 on SWC. When aggregated from 2007 to 2012, total six-year R_{eco} was stimulated by elevated CO_2 singly (24%) or in combination with warming (28%). Warming had little effect on annual R_{eco} under ambient CO_2, but stimulated it under elevated CO_2 (32% across all years) when precipitation was high (e.g., 44% in 2009, a 'wet' year). Treatment-level differences in R_{eco} can be partly attributed to the effects of antecedent SoilT and vegetation greenness on the apparent temperature sensitivity of R_{eco} and to the effects of antecedent and current SWC and vegetation activity (greenness modulated by VPD) on R_{eco} base rates. Thus, this study indicates that the incorporation of both antecedent environmental conditions and aboveground vegetation activity are critical to predicting R_{eco} at multiple timescales (subdaily to annual) and under a future climate of elevated CO_2 and warming.

Keywords: antecedent effects, carbon cycle, elevated CO_2, grasslands, soil respiration, temperature acclimation, warming

Received 11 August 2014; revised version received 17 December 2014 and accepted 25 January 2015

Introduction

Terrestrial plant and soil respiration, or ecosystem respiration (hereafter, R_{eco}), represents a major CO_2 flux in the global carbon cycle. Plant, root, and microbial respiration together account for approximately 118.7 Gt C yr^{-1}, which is ~95% of the carbon that is assimilated through photosynthesis (Roy *et al.*, 2001; Friedlingstein *et al.*, 2006; Canadell *et al.*, 2007; Beer *et al.*, 2010; Harmon *et al.*, 2011; Arora *et al.*, 2013). Although ecosystem respiration is a major component of the global carbon cycle, the effects of elevated atmosphere CO_2 and warming on R_{eco} remain uncertain. In particular, soil respiration accounts for ~90% of R_{eco} in temperate grasslands, and the influence of global change on this component of the global carbon budget is poorly constrained (Xiao *et al.*, 2003; Pendall *et al.*, 2004; Williams *et al.*, 2005; Hui *et al.*, 2008). Thus, global change experiments provide critical data to help constrain predictions of future changes in soil and ecosystem respiration, both of which are expected to have a large impact on the medium- to long-term carbon sequestration potential of the terrestrial biosphere.

The effect of warming on soil and ecosystem respiration is difficult to predict (Cox *et al.*, 2000; Davidson *et al.*, 2006), and the results from warming studies are often contradictory and vary according to biome and latitude. For example, a meta-analysis of 306 studies conducted between 1989 and 2008 found that soil respiration was generally positively correlated with increasing air temperature, although there was much variation in the strength of this relationship (Bond-Lamberty & Thomson, 2010). Conversely, a different meta-analysis found no consistent effects of temperature on soil

Correspondence: Edmund M. Ryan, tel. 480 727 3731, fax 480 965 6899, e-mail: emryan2@asu.edu
For submission to: *Global Change Biology*

respiration across 17 experimental warming studies, and in three grassland sites, factors other than warming explained differences in soil respiration (Rustad *et al.*, 2001). Other factors that drove soil respiration responses to warming included changes in growing season length, enhanced nutrient availability, shifts in species composition, and altered soil water, many of which are generally not accounted for in terrestrial carbon cycle models (Luo, 2007).

In contrast to the inconsistent effects of warming, elevated CO_2 has been shown to stimulate various components of R_{eco}, including soil respiration, in many ecosystems (Dieleman *et al.*, 2012). For example, in a deciduous temperate forest in eastern Tennessee, USA, elevated CO_2 stimulated heterotrophic respiration (by 10% over three years) and total soil respiration (nearly 40% over 1.5 years) in a FACE (Free Air and CO_2 Enrichment) study and an open-top chamber experiment (Norby *et al.*, 2002; Wan *et al.*, 2007), respectively. Elevated CO_2 also simulated soil respiration (by 20% over seven years) at a pine forest FACE site in North Carolina, USA (Bernhardt *et al.*, 2006). Similarly, in a semiarid Colorado grassland, soil respiration increased under elevated CO_2 by ~25% in a wet year and ~85% in a dry year (Pendall *et al.*, 2003). This CO_2 stimulation effect has been attributed to enhanced decomposition following increased substrate availability and soil moisture, increasing both autotrophic and heterotrophic components of soil respiration (Adair *et al.*, 2011; Pendall *et al.*, 2013).

Terrestrial ecosystem models require accurate representations of the interacting effects of climate change, yet the coupled belowground–aboveground responses underlying R_{eco} are poorly documented. Applying the ORCHIDEE model to data from 108 sites over a 20-year period, Piao *et al.* (2008) found that warming had a large positive effect on R_{eco} in the autumn and a small positive effect in the spring at northern high latitudes. The effects of warming, however, can be mediated by precipitation, with profound effects on terrestrial carbon fluxes. For example, Ciais *et al.* (2005) found that R_{eco} decreased by 77 gC m^{-2} yr^{-1} (~12%) across Europe as a result of rainfall deficit and extreme summer heat during the European heat wave of 2003. This decrease in R_{eco} was attributed to reductions in gross primary production and heterotrophic respiration, both of which were primarily driven by reductions in soil water content.

To accurately describe and predict the effects of climate change on R_{eco}, models should incorporate aboveground processes and antecedent factors as drivers of belowground responses (Reichstein *et al.*, 2003; Högberg & Read, 2006; Bardgett, 2011). For instance, shading and tree girdling experiments demonstrate the importance of photosynthesis drivers (e.g., light) for soil respiration (Craine *et al.*, 1999; Högberg *et al.*, 2001; Högberg & Read, 2006). Moreover, R_{eco} is very responsive to the effects of past conditions, such as antecedent soil water content or lagged precipitation (Huxman *et al.*, 2004; Xu *et al.*, 2004; Harper *et al.*, 2005; Chou *et al.*, 2008; Dezi, 2011; Oikawa *et al.*, 2014). For example, soil respiration was enhanced following a rain event, especially if the previous week or month was dry (Xu *et al.*, 2004; Cable *et al.*, 2008; Barron-Gafford *et al.*, 2014). These antecedent effects, however, can vary across diurnal, weekly, and monthly timescales (Vargas *et al.*, 2011; Cable *et al.*, 2013). In general, above- and/or belowground antecedent environmental conditions can explain spatial variation in soil respiration or R_{eco} (Barron-Gafford *et al.*, 2014; Oikawa *et al.*, 2014) and are likely to interact with elevated CO_2 and warming (Polley *et al.*, 2013).

Many studies have documented the singular effects of elevated CO_2 and warming (Rustad *et al.*, 2001; Norby & Zak, 2011), but these factors are expected to interact to affect R_{eco}, and the outcome of those interactions is unclear (Pendall *et al.*, 2004). Multifactor experiments that evaluate combined effects of elevated CO_2 and warming on soil and ecosystem respiration in natural ecosystems are rare, especially over longer timescales (Dieleman *et al.*, 2012). We addressed this knowledge gap by asking the following questions: (i) What are the consequences of warming, elevated CO_2, and altered soil moisture for R_{eco} over annual and multiyear timescales? (ii) How important are current and antecedent environmental factors (e.g., soil water and soil temperature) for understanding variation in R_{eco} and its long-term response to warming and elevated CO_2? Likewise, (iii) how important are aboveground factors (e.g., indices of plant activity) for predicting variation in R_{eco} and its response to warming and elevated CO_2?

To rigorously address our research questions, we conducted a unique analysis involving six years of R_{eco} data and associated below- and aboveground covariates generated from a multifactor global change experiment conducted in a mixed-grass prairie in Wyoming. We employed a novel Bayesian statistical analysis that analyzed these data in the context of a semi-mechanistic model, and which simultaneously quantified the potential impacts of elevated CO_2 and warming on the base rate (i.e., R_{eco} at a given temperature) and the apparent temperature sensitivity of R_{eco}. The model structure also allowed us to explore how CO_2 and warming interacted with antecedent soil water, antecedent temperature, and aboveground indices of vegetation activity to affect R_{eco} and its component

responses. Moreover, the hierarchical Bayesian framework was constructed to accommodate the experimental design, to allow for a rigorous quantification of the antecedent effects, and to propagate uncertainty in our model and parameter estimates to obtain realistic estimates of annual CO_2 efflux.

Materials and methods

Site description

The Prairie Heating and CO_2 Enrichment experiment is located in a temperate, mixed-grass prairie near Cheyenne, Wyoming (elevation = 1930 m). The site has a semiarid climate, characterized by moderately long winters and relatively warm summers. Mean monthly temperature varies from −2.5 °C in January to 17.5 °C in July, and mean annual precipitation is 384 mm (Morgan *et al.*, 2011). Over 75% of the vegetation cover consists of the C_3 grasses western wheatgrass (*Pascopyrum smithii* (*Rydb.*) *A. Löve*) and needle-and-thread grass (*Hesperostipa comata Trin and Rupr*), and the C_4 perennial grass blue grama (*Bouteloua gracilis* (*H.B.K.*) *Lag*). The soil is a fine-loamy, mixed, mesic Aridic Argiustoll, and biological crusts are not present (Bachman *et al.*, 2010).

Experimental design

The PHACE experiment involves an incomplete factorial design with 30 plots randomly assigned to six treatments, with five plots per treatment level (Parton *et al.*, 2007). The circular plots (3.4 m diameter) are separated from surrounding soil by a plastic flange buried to a depth of 60 cm (Bachman *et al.*, 2010). The six treatments – denoted as ct, cT, Ct, CT, ct-d, and ct-s – involve different combinations of atmospheric CO_2 [ambient at 380–400 ppm (denoted as 'c') vs. elevated at 600 ppm ('C')], temperature [ambient/not heated ('t') vs. heated by 1.5 (day) or 3.0 (night) °C ('T')], and watering [none vs. shallow ('s') or deep ('d') irrigation, which are only applied under ambient CO_2 and temperature ('ct')]. The goal of the irrigation treatments was to increase soil moisture to approximately match that of the Ct plots by irrigating when soil moisture fell below 85% of Ct at 5–25 cm depth. In 2007, the shallow irrigation plots received an equivalent of 18 mm of precipitation on 5 irrigation dates in 2007, the equivalent of 90 mm of additional growing season precipitation. From 2008 to 2011, irrigated plots received an equivalent of 21 mm of precipitation three times during the growing season (equivalent to 63 mm of additional precipitation), and in 2012, 65 mm of water was added four times during the growing season (equivalent to 260 mm). The ct-d plots were irrigated with the same total amount as the ct-s plots received the previous summer, but applied in fall and spring. Free Air CO_2 Enrichment (FACE) technology (Miglietta *et al.*, 2001) was used to raise atmospheric CO_2 to 600 ppm in the Ct and CT plots. A ceramic heater system using a proportional–integral–derivative (PID) feedback loop (Kimball, 2005) was used to raise temperatures in the cT and CT plots.

Data description

All data were measured in the field from 2007 to 2012 and consisted of R_{eco} (μmol m^2 s^{-1}), associated soil temperature (SoilT), volumetric soil water content (SWC), and aboveground factors consisting of ecosystem phenology ('greenness'), photosynthetically active radiation (PAR), air temperature, and relative humidity. One R_{eco} chamber frame was established in each plot, and R_{eco} was measured on 96 days over six growing seasons, each spanning the period between May and September. Measurement days were typically separated by 2–4 weeks; approximately every 6 weeks, R_{eco} was measured using a canopy gas exchange chamber (Jasoni *et al.*, 2005; Bachman *et al.*, 2010) five times during the day in each plot (nominal times = 04:00, 09:00, 12:00, 16:00 and 21:00); otherwise, a single plot-level measurement was made at midday. Soil thermocouples were installed at depths of 3 and 10 cm to record hourly SoilT (type-T thermocouples). SWC was measured at a depth of 5–15 cm on an hourly basis (EnviroSMART probe; Sentek Sensor Technologies, Stepney, Australia), but daily averages were computed for this analysis because, with the exception of days receiving precipitation, SWC showed little diurnal variation, and R_{eco} measurements were not made around precipitation events. A weather station at the site recorded air temperature, relative humidity, and PAR. Vegetation greenness was quantified every 2–4 weeks between March and October, resulting in 71 separate greenness measurement days spanning 2007–2012; photographs were taken for all 30 plots on each measurement day using a 2-m-high camera stand and a 1-m^2 ground frame. SAMPLEPOINT software (Booth *et al.*, 2006, www.samplepoint.org) was used to quantify parts of the photograph that were not vegetation (i.e., soil or litter) and to classify the different species of grass. Greenness (Gness) was quantified by converting the image pixels within each photograph to a matrix of numbers using MATLAB R2011a and quantifying the hue, saturation, and value scales for the detection of green. It varies from 0 (absence of green biomass) to 1 (plot is completely covered with green biomass). See Zelikova *et al.* (accepted) for full details on how greenness was quantified.

Gap-filling of environmental data

The SWC, SoilT, and micrometeorological data had occasional missing time periods or days due to instrument failure (<1%, 6%, and 2.5% for the micrometeorological, SWC, and SoilT data, respectively). We primarily used data from a nearby plot of the same treatment to gap-fill soil moisture and temperature, and cubic spline interpolation was used to gap-fill the missing micrometeorological data. Since the dates when repeat plot photographs were taken for vegetation greenness did not coincide with days when R_{eco} was measured, linear interpolation was employed to estimate greenness on R_{eco} measurement days. See Appendix S1 for full details of these gap-filling procedures.

Data synthesis and modeling

We synthesized the R_{eco} data in the context of a nonlinear mixed effects model that allowed us to quantify how the

experimental treatments influenced R_{eco}, and how they interacted with current and antecedent SoilT, SWC, and aboveground factors (e.g., vegetation greenness) to affect different properties of the R_{eco} response. Given the distributional properties of the observed R_{eco} data (i.e., $R_{eco} > 0$ and variance often increased with mean) and previous studies (Cable *et al.*, 2008, 2011, 2013), we assumed that the observed R_{eco} data (R_{eco}^{obs}) follow a log-normal distribution such that for treatment t ($t = 1, \ldots, 6$) and measurement time i [$i = 1, \ldots, N_t$, where N_t is the number of observations for treatment t, which varied from 531 (Ct) to 659 (ct-d)]:

$$\log(R_{eco_{i,t}}^{obs}) \sim \text{Normal}(\mu LR_{i,t}, \sigma_{LR}^2) \quad (1)$$

where μLR is the mean or predicted $\log(R_{eco})$ and σ_{LR}^2 represents the observation variance.

Note that time i represents a specific day (d) and hour (h) of the experiment for convenience, except when it is necessary to explicitly specify the corresponding day and hour.

We employ a semi-mechanistic, nonlinear process model for μLR that is a modification of an Arrhenius-type temperature function (Lloyd & Taylor, 1994). On the log scale, μLR is

$$\mu LR_{i,t} = LRb_{i,t} + E_{o_{i,t}}\left(\frac{1}{283.15 - T_{o_t}} - \frac{1}{SoilT_{i,p} - T_{o_t}}\right) \quad (2)$$

where $R_{base_{i,t}} = \exp(LRb_{i,t})$ is the base respiration rate at 10 °C (283.15 Kelvin), E_o is analogous to an energy of activation, but when Eqn (2) is applied to field observations of R_{eco}, E_o provides an index of the apparent temperature sensitivity of R_{eco} (Davidson & Janssens, 2006; Sierra, 2012). The interpretation of T_o is less straightforward, but it is also related to apparent temperature sensitivity, and we allow T_o to vary by treatment level. Soil temperature was measured at two depths (3 and 10 cm), and SoilT was estimated as a weighted average of each depth's temperature, with w_t and $(1 - w_t)$ representing the treatment-specific relative importance (weight) of the 3 and 10 cm depths, respectively; w_t is a parameter to be estimated.

We specify linear mixed effects models for $R_{base_{i,t}}$ and $E_{o_{i,t}}$ to incorporate the potential influence of current and antecedent soil and aboveground drivers on these two components of the R_{eco} response. For example, antecedent SWC (SWC_{ant}) has been found to significantly affect soil respiration in arid systems (Cable *et al.*, 2008, 2013; Barron-Gafford *et al.*, 2014), and the inclusion of antecedent soil temperature ($SoilT_{ant}$) allows for the apparent temperature sensitivity (E_o) to acclimate to prevailing temperature conditions (Luo *et al.*, 2001). The importance of including aboveground (ABG) factors for predicting R_{eco} and/or E_o has been highlighted in several places (Reichstein *et al.*, 2003; Högberg & Read, 2006; Bardgett, 2011), in particular, PAR (Craine *et al.*, 1999), vapor pressure deficit (VPD) (Carbone *et al.*, 2008; Cable *et al.*, 2013), indices of vegetation activity or greenness (Pendall *et al.*, 2001; Cable *et al.*, 2012), and photosynthetic activity (Drake *et al.*, 2011; Barron-Gafford *et al.*, 2014). We did not measure photosynthesis on the R_{eco} measurement days, but we incorporated proxies of aboveground plant activity in two ways: (i) A main effect of vegetation greenness (Gness) was included such that aboveground activity was assumed to be proportional to Gness, and (ii) interactions between Gness, VPD, and PAR were included, reflecting potential controls of these environmental factors on photosynthesis. Thus, E_o is given by

$$E_{o_{i,t}} = \alpha_{0,t} + \alpha_{1,t}SWC_{i,t} + \alpha_{2,t}SWC_{ant_{i,t}} + \alpha_{3,t}SWC_{i,t} \times SWC_{ant_{i,t}} + \alpha_{4,t}SoilT_{ant_{i,t}} + ABG_{i,t} + \epsilon_{plot} \quad (3)$$

$$ABG_{i,t} = (\alpha_{5,t}PAR_{ant_{i,t}} + \alpha_{6,t}VPD_{ant_{i,t}} + \alpha_{7,t}PAR_{ant_{i,t}} \times VPD_{ant_{i,t}}) \times Gness_{i,t} + \alpha_{8,t}Gness_{i,t} \quad (4)$$

where ε_{plot} represents a plot random effect. The expression for $LRb_{i,t}$ is the same as that of $E_{o_{i,t}}$, except that there is no $SoilT_{ant_{i,t}}$ term, and it has its own set of parameters, labeled $\beta_0, \ldots, \beta_7$, with β_4–β_7 corresponding to the aboveground effects in Eqn (4).

Quantification of antecedent drivers

We employ a novel stochastic modeling approach (Ogle *et al.*, 2015) to define the antecedent driving variables, as adopted by Cable *et al.* (2013) and Barron-Gafford *et al.* (2014). This new approach differs from a more 'standard' approach that computes the antecedent variables prior to the data analysis, often by averaging the daily or hourly variables over a specified time period. Here, we allow the R_{eco} data to determine the relative importance of each variable at different past time periods. Based on exploratory analyses, and following Cable *et al.* (2013), we assumed that R_{eco} was influenced by SoilT and the aboveground covariates over daily timescales and by SWC over weekly timescales that integrate over past precipitation events. Thus, VPD_{ant}, PAR_{ant}, and $SoilT_{ant}$ were modeled as weighted averages of the corresponding observed daily values over the past seven days; likewise, SWC_{ant} was modeled as a weighted average of the observed weekly SWC over the past 10 weeks. Let X denotes one of the daily timescale variables (X = VPD, PAR, or SoilT); we first computed the 24-h means for each variable ($\bar{X}$) based on the observed hourly values. The antecedent variable (X_{ant}) is expressed as a weighted average of the past daily mean values such that for an R_{eco} observation made on plot p and at time i:

$$X_{ant_{i,p}} = \sum_{k=1}^{Nperiods} W_{X_{k,p}} \bar{X}_{tp(i)-k,p} \quad (5)$$

where $tp(i)$ represents the 24-h time period associated with R_{eco} observation i. For example, if an observation of R_{eco} was made at 9:00 am on day 10, then the associated tp covers 9:00 am on day 9 to 9:00 am on day 10; $k = 1$ refers to the previous 24-h time period (e.g., 9:00 am day 8 to 9:00 am day 9), and similar for $k = 2, 3, \ldots, N_{periods}$. VPD_{ant} and PAR_{ant} are not indexed by p as these data are site specific rather than plot specific. We do not specify the values for the weights (W_X) as they are parameters to be estimated. The formula for SWC_{ant} is similar to Eqn (5) except that the time period ($k = 1, \ldots, N_{periods}$) is on the weekly scale. To reduce the number of weights associated with SWC_{ant}, we assigned individual weights to each of the first four weeks into the past, the fifth

weight to past weeks 5 and 6, and the sixth weight to past weeks 7–10.

Bayesian framework and prior distributions

The above model is nonlinear because it is based on the Arrhenius-type temperature–response function, with mixed effects associated with the plot random effects and fixed effects for the different treatment levels and for the continuous environmental and aboveground covariates. We fit this model via a hierarchical Bayesian framework to accommodate the nonlinear model and the experimental design, and to explicitly estimate sources of variability due to observation error, model or process error, and parameter uncertainty (Clark, 2003; Ogle & Barber, 2008; Cressie *et al.*, 2009; Parslow *et al.*, 2013). This approach produces posterior distributions for all stochastic quantities of interest, and we summarize their marginal posteriors by reporting posterior means, 95% credible intervals (CIs), and Bayesian *P*-values (Gelman *et al.*, 2003).

The Bayesian approach also allows us to incorporate prior information. For example, based on the extensive synthesis conducted by Lloyd & Taylor (1994) on the response of soil respiration to temperature, we constructed semi-informative priors for α_0 [base rate parameter of E_o in Eqn (3)] and T_o [Eqn (2)]. Specifically, we assumed $\alpha_{0,t}$ ~ Normal(308.56,1000) and T_o ~Normal(227.13,1000). Lloyd & Taylor (1994) also state that T_o can only lie between 0 K and the minimum observed SoilT; thus, the Normal prior for T_o was also truncated to the interval [0, 261]. With no specific information on the parameters α_1–α_8 and β_0–β_7 in Eqns (3) and (4), independent and diffuse Normal distributions were used as priors for each. The plot-level random effects [ε's, Eqn (3)] for the E_o and LRb functions were assigned normal priors with a zero mean and variances given by ${\sigma_1}^2$ and ${\sigma_2}^2$ for E_o and LRb, respectively. Uniform priors were assigned to the standard deviations, including that associated with the observation error in Eqn (1), such that σ_k ~U(0,150) (k = 1,2) and σ_{LR} ~U(0,10). Dirichlet priors were used for the vectors of antecedent weights in Eqn (5), thus obeying the constraint that the W_X's must sum to one across past time periods (k = 1, . . ., $N_{periods}$) and ensuring that $0 \leq W_{X\,k} \leq 1$ for all variables X, treatment levels t, and times into the past k.

Alternative model formulations

We refer to the above model as the 'main' model. Two other models were implemented evaluate the importance of including antecedent and/or aboveground effects. The first alternative model did not include any of the aboveground covariates [i.e., the ABG term was excluded in Eqn (3)], while the other model did not include any antecedent covariates [i.e., all terms with a subscript 'ant' in Eqns (3) and (4) were removed]. A fourth model that included an extra term in Eqn (2) to account for day random effects, in addition to plot random effects, was also considered. As the predicted day random effects showed no temporal structure, this model was not included in our final analysis.

Model implementation and assessment

We used the software package OPENBUGS (Lunn *et al.*, 2009) to implement the Bayesian analysis of the main model and the three model variants. OPENBUGS uses Markov chain Monte Carlo (MCMC) techniques to sample from the joint posterior of the model parameters, and we ran three parallel chains for each model. Depending on the model, the number of iterations per chain varied from 50 000 to 550 000, with the first 1000–50 000 iterations discarded as burn-in, and the amount of thinning ranged from every 10th to 500th iteration to sufficiently reduce autocorrelation in the chains and to reduce storage requirements. This produced 3000 independent samples from the posterior distribution for each parameter, for each model. Convergence was assessed using the built-in Brooks–Gelman–Rubin diagnostic tool (Gelman *et al.*, 2003).

We assessed the ability of each model to fit the observed R_{eco} data by plotting observed vs. predicted R_{eco} values. The coefficient of determination (R^2) and the coefficients of the corresponding regression line give an informal evaluation of replicative performance (i.e., 'goodness of fit'). We also computed posterior predictive loss (D), a model comparison statistic, which is the sum of a goodness-of-fit term (G) and a model complexity penalty term (P) (Gelfand & Ghosh, 1998). One model is more desirable over another if it has a lower D value, which can result from a lower G value (better fit) and/or a lower P value (less complex).

Estimates of annual R_{eco}

We used the posterior results from the main model to obtain hourly estimates of R_{eco} for each treatment level. This was accomplished by sampling model parameters from their joint posterior distribution and computing hourly, treatment-level R_{eco} based on Eqns (2)–(5), with ε_{plot} = 0, and given hourly observations of the covariates (i.e., SWC, SoilT, Gness, VPD, PAR). These hourly values were summed to obtain posterior predictive distributions of treatment-level daily and annual (March–October) R_{eco}. The annual estimates were also summed to obtain predicted annual R_{eco} over the six-year study period.

Moreover, the majority of models do not include antecedent variables in R_{eco}. To quantify the effect of ignoring antecedent conditions, we also computed annual and 6-year R_{eco} sums based on the model lacking antecedent effects [i.e., only had current SWC and Gness as covariates in Eqns (3) and (4)] and compared these estimates to those obtained from the main model (above).

Results

Assessment of model performance

The main model accurately predicted ecosystem respiration (R_{eco}) over the entire set of observations (R^2 = 0.77). However, the goodness of fit varied among the treatments, with R^2 ranging from 0.84 (cT) and 0.79 (ct) to 0.63 (CT) (Fig. 1). The treatment-level differences

in model fit are also illustrated in time series plots of observed vs. predicted log(R_{eco}) (see Fig. 2 for 2009 and Fig. S1a–e for remaining years). For any year, <5% of the observations fell outside of the predicted 95% credible intervals, and at least three quarters of these were underpredicted by the model, with the majority occurring between June and August. The inclusion of the aboveground and antecedent covariates was important for predicting R_{eco}, and exclusion of either notably reduced model fit (R^2 = 0.68 and 0.64, respectively) and increased posterior predictive loss. The likely reasons for the variations in model performance among treatments are discussed in the Appendix S2).

Treatment effects on R_{eco}

We assessed treatment effects on annual (March–October) ecosystem respiration values (Fig. 3). Elevated CO_2 increased annual ecosystem respiration (R_{eco}; Fig. 3; ct vs. Ct or cT vs. CT, Bayesian $P < 0.05$ in 2008, 2009, 2011 and 2012, $P < 0.10$ in 2007 and 2010). The combination of warming and elevated CO_2 stimulated R_{eco} compared to the control (Fig. 3) when aggregated over the six years (2007–2012, $P = 0.03$) and in five of the six years when considered individually ($P < 0.09$ in 2007, 2008 and 2009; $P < 0.04$ in 2011 and 2012). Recall that the shallow irrigation treatment (ct-s) was applied such that the soil water content (SWC) was roughly the same as that of the elevated CO_2 treatment (Ct); the deep irrigation (ct-d) applied was the same amount as the surface irrigation from the previous year. There was no difference ($P > 0.2$) in annual R_{eco} between the elevated CO_2 treatment and either irrigation treatment (Ct vs. ct-d or Ct vs. ct-s) for any of the years or when aggregated over the six-year period (Fig. 3). When compared to the control treatment, irrigation did enhance annual R_{eco} for three years (Fig. 3; $P = 0.03$ in 2007 for ct vs. ct-s, $P = 0.06$ in 2011 for ct vs. ct-d, $P = 0.001$ and 0.006 in 2012 for ct vs. ct-d and ct vs. ct-s, respectively).

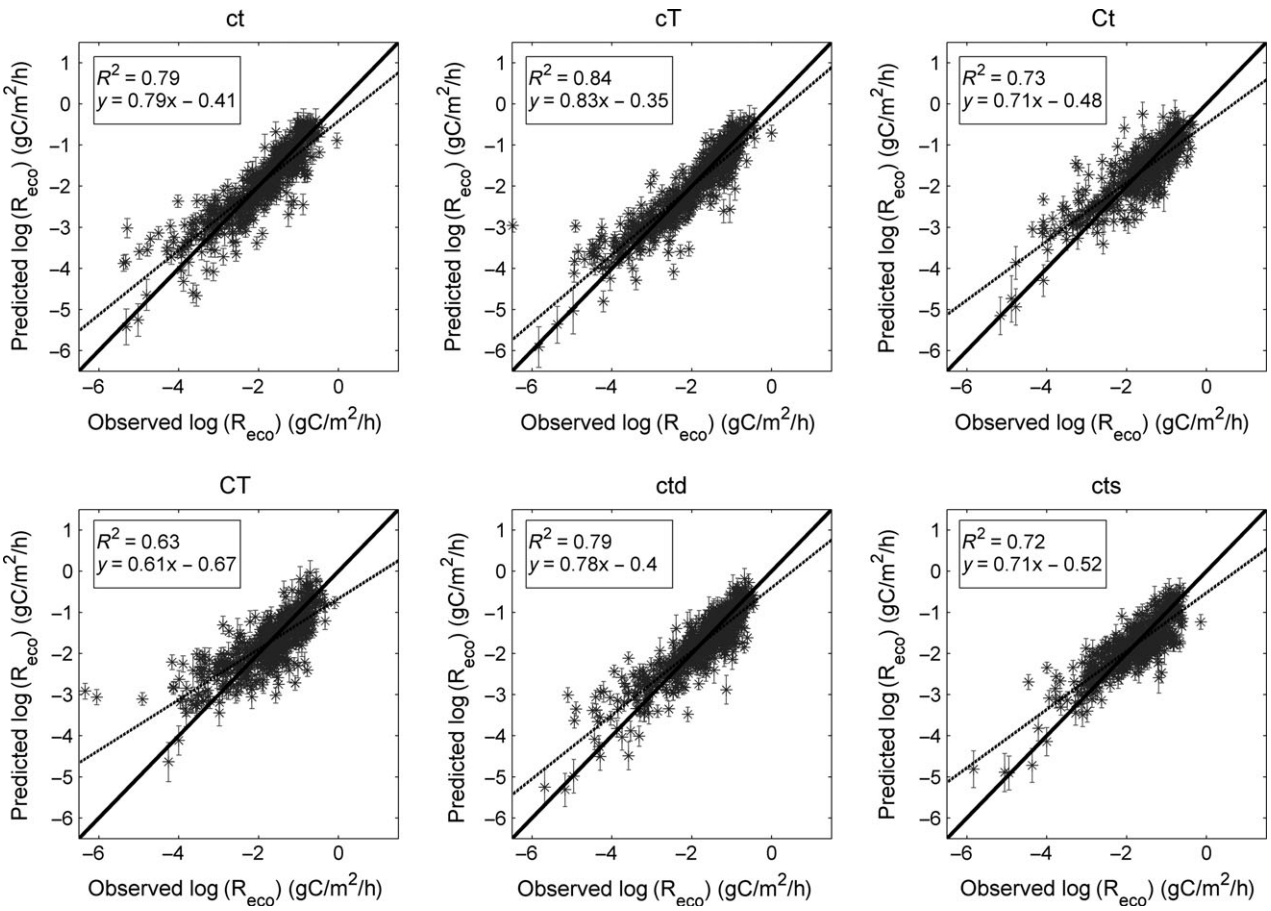

Fig. 1 Observed vs. predicted log(R_{eco}) for each treatment. The predicted values are the posterior means and central 95% credible intervals for replicated observations (Gelman *et al.*, 2013) of log(R_{eco}), based on Eqns (1) and (2). Treatments codes involve combinations of: c (ambient CO_2), C (elevated CO_2), t (no warming), T (warming), d (deep irrigation), or s (shallow irrigation).

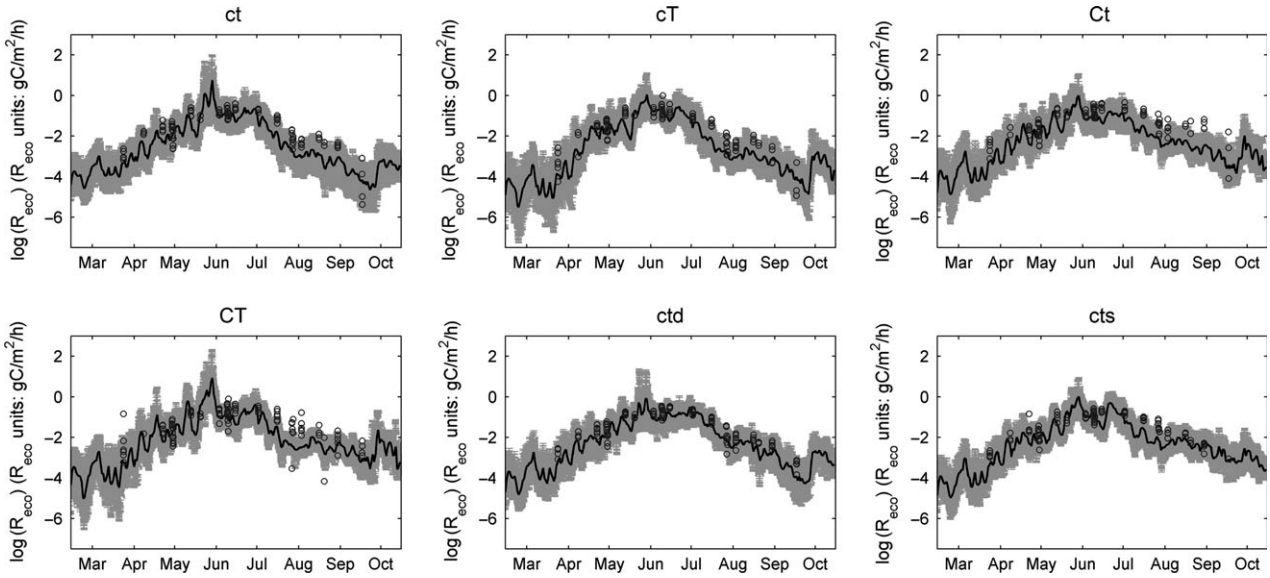

Fig. 2 Time series of predicted log(R_{eco}) for each treatment in 2009, represented by the posterior means for the daily values (black line) and central 95% credible intervals on the hourly time-scale (grey region). The circles denote observations of log(R_{eco}). See Fig. 1 legend for treatment codes. Time series for the other years are presented in Fig. S1a–e.

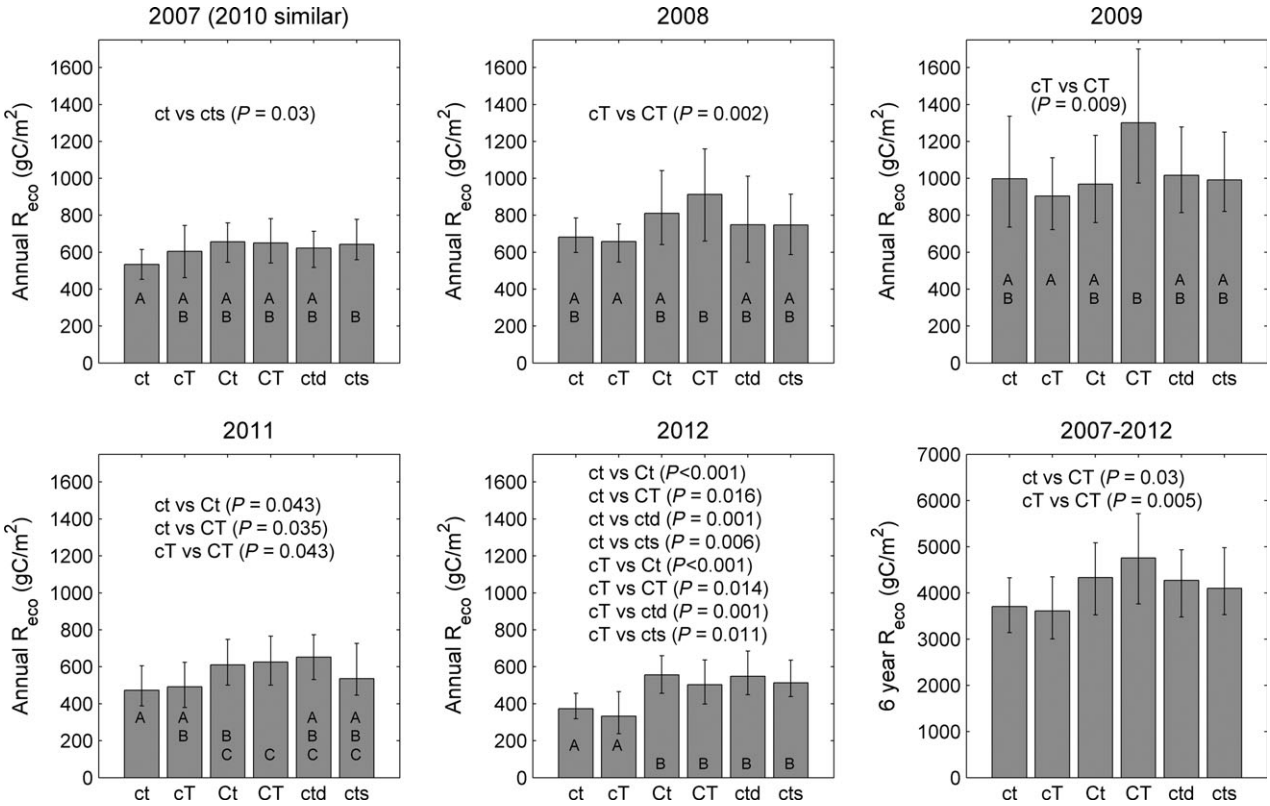

Fig. 3 Annual R_{eco} for each treatment and each study year and across all six years is shown. Bars denote the posterior means and the error bars represent the central 95% credible intervals. The letters inside the bars indicate statistically significant (at the 5% level) differences among treatments, and the Bayesian *P* values for significantly different treatment pairs are provided in each panel. The results for 2010 are not shown since they look very similar to the 2007 results. See Fig. 1 legend for treatment codes.

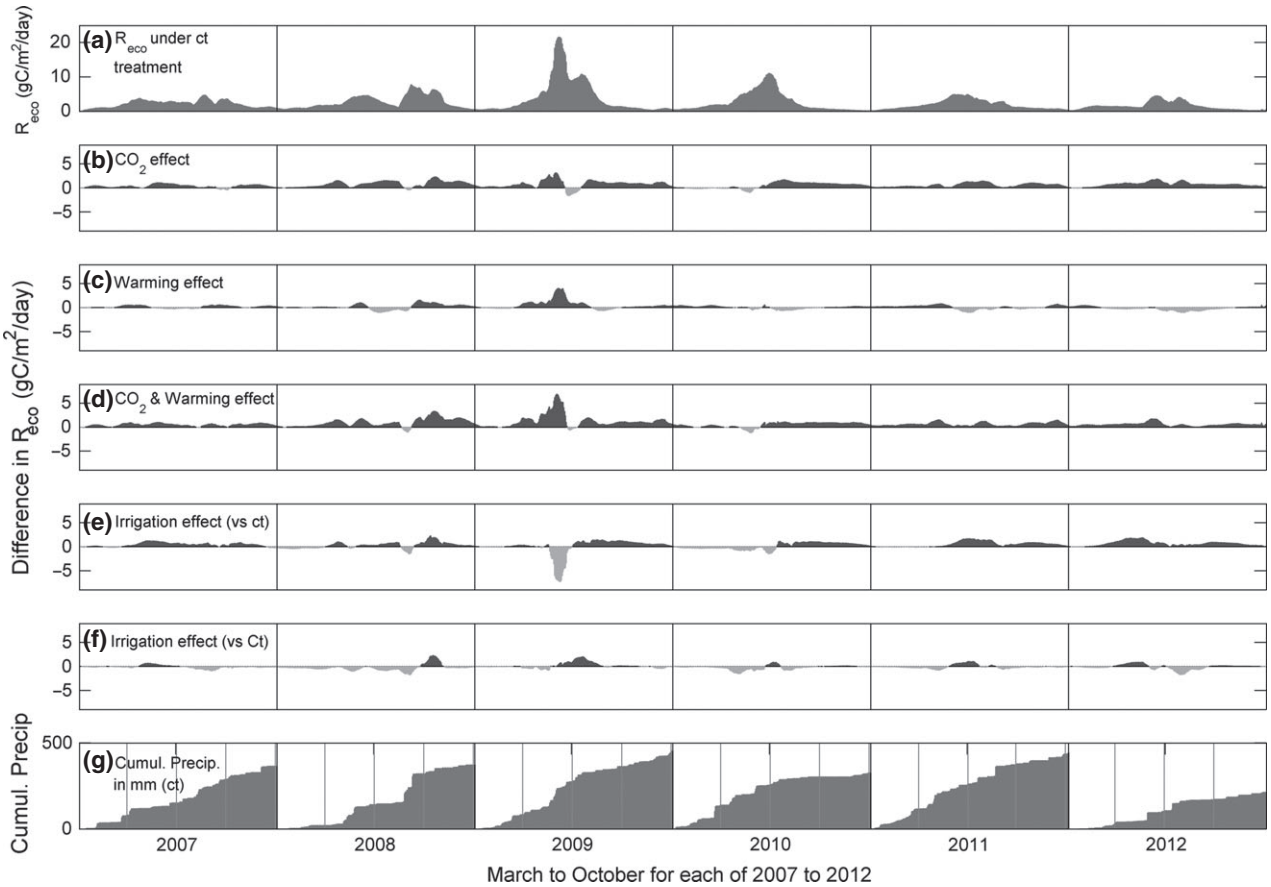

Fig. 4 Time-series of posterior means of daily contrasts to evaluate treatment-level differences in daily predicted R_{eco}. (a) Posterior means for daily R_{eco} under the ambient treatment (ct) are shown for reference. Five different treatment contrasts were computed: (b) effect of CO_2: (Ct+CT)/2 – (ct+cT)/2; (c) effect of warming: (cT+CT)/2 – (ct+Ct)/2; (d) combined CO_2 and warming effect: CT – ct; (e) effecting of watering relative to ambient conditions: (cts+ctd)/2 – ct; (f) effect of watering relative to elevated CO_2: (cts+ctd)/2 –Ct. For ease of presentation, the credible intervals are not shown. For panels (b)–(f), the dark grey region indicates a positive treatment effect, while the light grey region denotes a negative effect. Panel (g) shows the site level cumulative precipitation for each year.

We also evaluated treatment effects on R_{eco} over shorter timescales by assessing temporal changes in pairwise differences of daily R_{eco} for key pairs of treatments (Fig. 4). This analysis indicated that the daily predicted R_{eco} was consistently enhanced under elevated CO_2 (Fig. 4b). Warming increased and decreased R_{eco} by approximately equal amounts within each season, but there were no consistent seasonal trends. Furthermore, the magnitude of the warming response was substantially less than under elevated CO_2, except for the wettest year of 2009 where warming resulted in greater increases in R_{eco} (Fig. 4c). For 2009 only, the combined effect of warming and elevated CO_2 enhanced R_{eco} to a greater extent than singularly under elevated CO_2, but the effects of the two elevated CO_2 treatments (Ct and CT) were comparable for the remaining years (Fig. 4b vs. Fig. 4d). The R_{eco} daily differences between Ct and each of the two irrigation treatments (ct-s and ct-d) were not consistently positive or negative throughout the study period (Fig. 4f). In addition, for the irrigation treatments vs. ambient conditions (ct), the timing and magnitude of the irrigation effect (Fig. 4e) was similar to that of the CO_2 effect (Fig. 4b).

Importance of current and antecedent soil conditions for understanding treatment effects on R_{eco}

Increases in current soil water content (SWC) are expected to increase the respiration base rate (R_{base}), and this positive effect was similar for all treatments (Fig. 5d; Table 1, $P < 0.001$). By contrast, current SWC did not affect the apparent temperature sensitivity of R_{eco} (i.e., E_o), which was also consistent across treatments (Fig. 5a; Table 1). Antecedent soil water content and antecedent soil temperature, either singly (SWC_{ant} or $SoilT_{ant}$) or in combination with current conditions ($SWC \times SWC_{ant}$), were also important predictors of R_{eco}

Table 1 Summary of posterior estimates and Bayesian *P*-values for the effects parameters in the models for E_o (α parameters) and $\log(R_{base})$ (β parameters) [see Eqn (3)]. Black cells indicate $P \leq 0.001$, dark gray indicates $0.001 < P \leq 0.01$, light gray indicates $0.01 < P \leq 0.05$, and white indicates $P > 0.05$. The signs (+ or −) indicate whether an effect is positive or negative. For a particular effect parameter, the letters in the cells indicate significant treatment differences such that if two treatments do not share the same letter, $P < 0.01$ for the associated treatment difference. See Fig. 1 legend for treatment codes

Effect parameter	ct	cT	Ct	CT	ct-d	ct-s
α_1 (SWC)	A	A	A	A	A	A
α_2 (SWC_{ant})	A	A	A	A	A	A
α_3 ($SWC \times SWC_{ant}$)	A	A	A	A	A	A
α_4 ($SoilT_{ant}$)	− A	− AB	− B	− C	− BC	− AB
α_5 ($PAR_{ant} \times Gness$)	A	A	A	A	− A	A
α_6 ($VPD_{ant} \times Gness$)	A	A	+ B	AB	AB	AB
α_7 ($PAR_{ant} \times VPD_{ant} \times Gness$)	A	A	A	− A	A	A
α_8 (Gness)	+ AB	+ AB	+ AB	+ A	B	AB
β_1 (SWC)	+ A	+ A	+ A	+ A	+ A	+ A
β_2 (SWC_{ant})	+ AEF	+ AGH	+ BEI	CI	+ DFG	CH
β_3 ($SWC \times SWC_{ant}$)	− AB	− BC	− AB	− A	− CD	+ E
β_4 ($PAR_{ant} \times Gness$)	+ AB	A	+ AB	+ AB	+ B	AB
β_5 ($VPD_{ant} \times Gness$)	− A	AB	− B	− AB	− AB	− AB
β_6 ($PAR_{ant} \times VPD_{ant} \times Gness$)	+ A	A	+ A	+ A	+ A	A
β_7 (Gness)	A	A	A	A	+ A	+ A

(Table 1, gray and black squares). The importance of the $SWC \times SWC_{ant}$ term means that wet periods in the past (high SWC_{ant}) were associated with higher base respiration rates ($\beta_2 > 0$; Table 1); however, if a rain event occurred during a wet period, the response of R_{eco} to this increase in current SWC was dampened compared to the increase in R_{eco} following an event occurring during a dry period ($\beta_3 < 0$; Table 1).

Antecedent belowground effects on R_{eco} differed among treatments. Apparent temperature sensitivity (E_o) was reduced during warm periods ($\alpha_4 < 0$, Table 1), but the size of the reduction was larger for the elevated CO_2 treatments compared to the ambient treatments (Fig. 5b; ct vs. Ct or cT vs. CT, Bayesian $P = 0.013$ and $P < 0.001$, respectively). The respiration base rate (R_{base}) was enhanced as antecedent soil water increased (β_2), but the enhancement was less pronounced under elevated CO_2 (ct vs. Ct or cT vs. CT, $P = 0.01$ and $P < 0.001$, respectively). Under the combined effect of elevated CO_2 and warming relative to the control treatment, the changes in R_{eco} were most pronounced for every unit increase in either three of the belowground antecedent terms – antecedent soil water content (SWC_{ant}), the interaction between current and antecedent soil water content ($SWC \times SWC_{ant}$), and the antecedent soil temperature ($SoilT_{ant}$) – compared to increases in any of the other model terms ($P < 0.001$ for $SoilT_{ant}$, Fig. 5b; $P = 0.001$ for SWC_{ant}; $P = 0.02$ for $SWC \times SWC_{ant}$, Fig. 5e). These findings suggest that differences in annual R_{eco} among under elevated CO_2 and the combined effect of elevated CO_2 and warming (Fig. 3) are most likely driven by differential effects of antecedent soil water (SWC_{ant} and $SWC \times SWC_{ant}$) and antecedent soil temperature ($SoilT_{ant}$).

Importance of aboveground factors for understanding treatment effects on R_{eco}

The aboveground covariates – namely antecedent photosynthetically active radiation (PAR_{ant}), antecedent

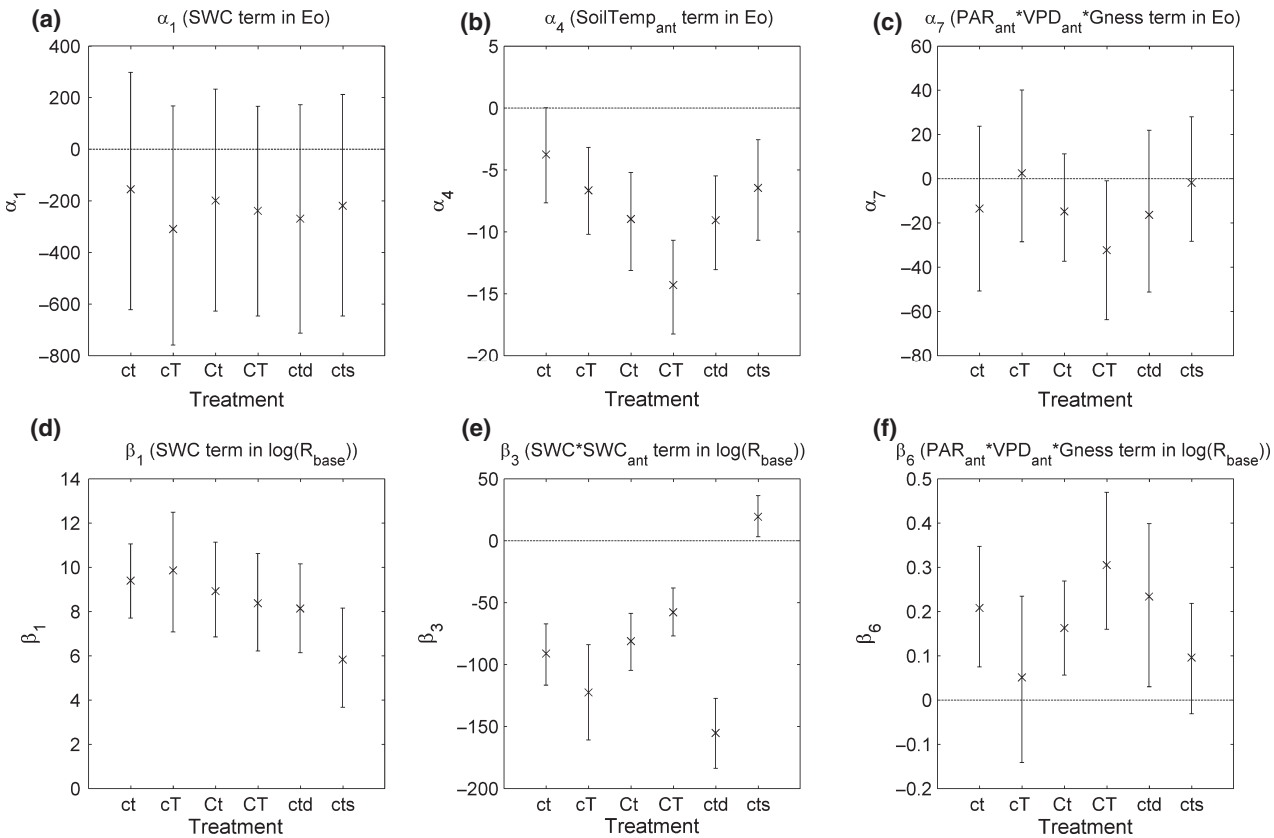

Fig. 5 Posterior means and central 95% credible intervals (CIs) of a subset of effects parameters in the E_o model (panels a–c) and the log(RE_{base}) model (panels d–f). Covariates shown include current soil water content (SWC), antecedent soil temperature ($SoilT_{ant}$), antecedent vapor pressure deficit (VPD_{ant}), vegetation greenness (Gness), and antecedent soil water content (SWC_{ant}). The dashed horizontal line represents zero, and 95% CIs that overlap with zero indicate a non-significant effect. See Fig. 1 legend for treatment codes.

vapor pressure deficit (VPD_{ant}), and vegetation greenness (Gness) – and their interactions [Eqn (4)] are important for predicting R_{eco} (Table 1, gray and black squares). However, their importance is less than those of the belowground covariates – namely current and antecedent soil water content and antecedent soil temperature (SWC, SWC_{ant}, and SWC*SWC_{ant}, $SoilT_{ant}$; Table 1). Aboveground covariates generally had greater influence on the R_{base} rather than the E_o component of R_{eco} (Fig. 5c,f; Table 1). Of the aboveground covariates, vegetation greenness was the most important one influencing the apparent temperature sensitivity of R_{eco} (E_o) such that increases in it increased the apparent temperature sensitivity of R_{eco}. However, the strength of the vegetation greenness effect on R_{eco} varied among treatments (Table 1). Conversely, vegetation greenness and its interactions with antecedent PAR and antecedent VPD were the most important predictors of the respiration base rate (R_{base}), suggesting that R_{base} is more strongly coupled to photosynthesis than to the amount of active vegetation present (vegetation greenness; Table 1). Although the direction (positive or negative) of each aboveground effect was consistent across treatments, the magnitude and relative importance of the effects of the aboveground factors on R_{base} varied among treatments. For example, the interactive effect of antecedent photosynthetically active radiation, antecedent vapor pressure deficit, and vegetation greenness ($PAR_{ant}\times VPD_{ant}\times$Gness) is positive for all six treatments (i.e., $\beta_6>0$, Table 1), but β_6 is more positive under the interaction of elevated CO_2 and warming (Fig. 5f).

Quantifying the timescales of the antecedent effects

The effect of antecedent vapor pressure deficit (VPD) on R_{eco} varied across time. Specifically, VPD conditions experienced the first three (of seven) days prior to the R_{eco} measurement were the most important for predicting R_{eco}; that is, these days were associated with the highest weights [W_X, Eqn (5)] for all treatments, with days 1 (yesterday) and 3 into the past having the greatest importance under the ct, CT, Ct, and CT treatments (Fig. S2). For the other three antecedent

covariates – namely antecedent soil water content, antecedent soil temperature, and antecedent photosynthetically active radiation (SWC_{ant}, $SoilT_{ant}$, and PAR_{ant}) – the weights tended to be indistinguishable across all treatments and past time periods (Fig. S2).

Consequences of not including antecedent effects

Excluding antecedent conditions from the R_{eco} model generally resulted in increases in the predicted, annual 6-year R_{eco}, increasing 3.9% under deep irrigation (ct-d), 7.7% under the control treatment (ct), ~10% under warming (cT) and elevated CO_2 (Ct), and 17.8% under surface irrigation (ct-s). The only exception was the combined CO_2 and warmed treatment (CT) treatment, where exclusion of antecedent effects resulted in a 3.6% reduction in the predicted 6-year R_{eco}.

Discussion

Consequences of warming, elevated CO_2, and altered soil moisture for R_{eco} over annual to multiyear timescales

Our Bayesian synthesis approach allowed us to *simultaneously* evaluate the importance of multiple environmental and biotic drivers at different timescales. Thus, our analysis provided insight into to annual and multiyear effects of global change treatments, seasonal, weekly, and daily effects of antecedent conditions and vegetation activity, and daily and subdaily effects of concurrent changes in above- and belowground environmental conditions on R_{eco}. The analysis also allowed us to partition the effects of these environmental and biotic factors on the apparent temperature sensitivity (E_o) vs. the respiration base rate (R_{base}), thus providing insights into potential mechanisms affecting R_{eco} over these different timescales. Additionally, our stochastic approach to incorporating antecedent covariates has been implemented in only a handful of very recent studies, and this approach is expected to provide more realistic inferences about the importance of past conditions.

Our model of hourly and annual R_{eco} suggests that annual R_{eco} is stimulated under elevated CO_2 in four of the six years of the PHACE experiment at the 5% level of statistical significance, resulting in an overall stimulation across the 2007-2012 study period. These findings are consistent with a recent PHACE study that used a linear interpolation technique to obtain annual R_{eco} sums for 2007–2010 (Pendall *et al.*, 2013), which reported elevated CO_2 effects under both ambient and increased temperature conditions. In contrast, we mainly found that elevated CO_2 stimulated R_{eco} only under warming. When warming was combined with elevated CO_2, R_{eco} increased across most of the duration of the PHACE experiment, but against our initial expectations, warming by itself did not significantly affect annual R_{eco}. This appears to be in contrast to the findings of Pendall *et al.* (2013), who showed a significant main effect of warming on annual R_{eco} for two (2007 and 2010) of the four years in their study. However, our results also suggest a trend toward the enhancement of R_{eco} under warming, but due to our more thorough error propagation, the associated higher uncertainty estimates resulted in fewer significant warming and elevated CO_2 effects. In particular, our method builds on the analysis of Pendall *et al.* (2013) by employing a more process-based modeling approach that quantifies the environmental drivers of R_{eco}, in addition to treatment effects. Such process-based models are recommended for gap-filling time series data (Desai *et al.*, 2008). Thus, we used our model to estimate hourly R_{eco} on nonmeasurement days, enabling us to represent daily and subdaily variation in R_{eco}. Furthermore, our Bayesian approach also allowed for the propagation of the uncertainty associated with these hourly estimates, thus providing potentially more realistic estimates of the range of possible annual R_{eco} values.

An important contribution of our analysis involving six years of data is that the effects of warming differed between wet and dry years. In a dry year (e.g., 2012), warming likely exacerbated soil water deficits (Ciais *et al.*, 2005; Morgan *et al.*, 2011), which led to lower R_{eco} in 2012 (Fig. 3). However, in a wet year, warming increased microbial activity and thus decomposition rates (Nie *et al.*, 2013), which helps to explain our predicted amplification of annual R_{eco} under both warming and elevated CO_2 in 2009 (Fig. 3). Aboveground biomass production was also higher in 2009 (Morgan *et al.*, 2011), likely paralleled by increased root respiration and potentially greater priming effects (Carrillo *et al.*, 2011), which together would enhance overall higher R_{eco}.

The importance of moisture for annual R_{eco} can also be inferred by evaluating the effects of the irrigation treatments. The main goal of applying the shallow irrigation treatment was to determine whether the stimulation of R_{eco} under elevated CO_2 was the direct result of elevated CO_2 or an indirect effect of an increase in soil water content (SWC) associated with elevated CO_2 due to, for example, higher plant water-use efficiency under elevated CO_2 (Pendall *et al.*, 2003). Annual R_{eco} did not differ between elevated CO_2 and watered plots, suggesting that elevated CO_2 indirectly stimulated R_{eco} via a positive effect on SWC. However, for all but two years, annual R_{eco} also did not differ between watered and ambient CO_2 plots, suggesting that such water

savings is likely only one of several factors that can influence R_{eco} under elevated CO_2; other potential factors are increases in root biomass (Carrillo *et al.*, 2014), labile C pools (Carrillo *et al.*, 2011), or priming of soil organic matter decomposition (Nie *et al.*, 2013).

Importance of current and antecedent soil water and temperature for understanding variation in R_{eco} and its long-term response to warming and elevated CO_2

Overall, water availability was critical for most aspects of R_{eco}. For example, averaging across treatments, annual R_{eco} was positively correlated with total annual precipitation (Fig. S3); variation in this relationship points to the importance of the seasonal distribution of precipitation (Huxman *et al.*, 2004; Cable *et al.*, 2008; Patrick *et al.*, 2009) and legacy effects of past precipitation (Schwinning *et al.*, 2004). For example, 2008 had the second-lowest annual precipitation, but the second-highest annual R_{eco}. Most of the precipitation in 2008 was delivered in two large storms (one in June, one in September) that occurred after 2–3 months of virtually no precipitation, and the timing of daily R_{eco} peaked corresponded to the timing of these two events (Fig. 4g). This confirms other reports of exceptionally large enhancements of ecosystem and soil CO_2 fluxes following rain events that break long dry spells in arid ecosystems (Xu *et al.*, 2004; Sponseller, 2007; Cable *et al.*, 2008, 2011; Thomas *et al.*, 2008) and also highlights the importance of past precipitation patterns for predicting R_{eco}. Moreover, although 2010 was one of the driest study years, it had the third-highest annual R_{eco}, suggesting a legacy effect of the preceding wet year on R_{eco} as well as plant production (Nippert *et al.*, 2006; Ogle *et al.*, 2015).

The antecedent effects in our model represent legacy effects over shorter timescales (e.g., daily to weekly), and most antecedent covariates affected R_{eco} similarly across the different global change treatments. For example, the directions (positive or negative) of the antecedent soil water effect on R_{eco} were the same across all six treatments (Table 1). Increases in current or antecedent SWC (SWC_{ant}) have been shown to stimulate R_{eco} (Davidson *et al.*, 1998), but we also found a negative interaction between current and antecedent SWC (Table 1), which is consistent with other studies of soil or ecosystem respiration in semiarid grasslands (Huxman *et al.*, 2004; Xu *et al.*, 2004; Harper *et al.*, 2005; Chou *et al.*, 2008) and deserts (Xu *et al.*, 2004; Sponseller, 2007; Cable *et al.*, 2008, 2011; Thomas *et al.*, 2008; Barron-Gafford *et al.*, 2014; Oikawa *et al.*, 2014). This negative interaction indicates that increased SWC stimulates a greater R_{eco} response if the rain event occurs during a dry vs. wet period. Under extremely wet conditions (very high SWC_{ant}), it is possible that a rain event could reduce R_{eco}, potentially reflecting oxygen limitations of respiration (Skopp *et al.*, 1990; Davidson *et al.*, 2012) or constraining the diffusivity of CO_2 (Moldrup *et al.*, 2004). Interestingly, our analysis suggests that SWC and SWC_{ant} only affect R_{eco} through their effects on the base rate (R_{base}), whereas other studies (Cable *et al.*, 2011, 2013; Barron-Gafford *et al.*, 2014) suggest that soil water conditions also affect the apparent temperature sensitivity of R_{eco}.

Consistent across all six treatments, antecedent soil temperature ($SoilT_{ant}$) most strongly affected the apparent temperature sensitivity (E_o) of R_{eco}, a trend suggestive of a Type I temperature acclimation response (Atkin & Tjoelker, 2003) that can be amplified by long-term warming (Luo *et al.*, 2001; Davidson *et al.*, 2006; Tucker *et al.*, 2013). For example, under elevated CO_2 and warming (CT), this temperature acclimation response was significantly stronger ($SoilT_{ant}$ parameter was more negative) than under the control treatment (ct) (Fig. 5b). In opposition to this finding, the 6-year R_{eco} sum was significantly greater under CT (Fig. 3), which can be explained by R_{base} being significantly greater under CT compared to ct, indicating that acclimation of E_o was more than compensated by enhanced R_{base} in the CT treatment. This enhancement of R_{eco} under the combined effect of elevated CO_2 and warming agrees with findings from a laboratory incubation experiment using soil microbes from the same site (Nie *et al.*, 2013). We speculate that the soil organic matter priming mechanism (Pendall *et al.*, 2003; Dijkstra *et al.*, 2013), which would most likely affect R_{base} more than E_o, may be more important than the direct effects of temperature change for understanding positive climate-CO_2 feedbacks (Cox *et al.*, 2000; Luo, 2007; Luo *et al.*, 2008).

Importance of aboveground factors for understanding variation in R_{eco} and its long-term response to warming and elevated CO_2

Our results suggest that vegetation greenness was an important predictor of R_{eco} by affecting the base rate (R_{base}), especially when interacting with antecedent vapor pressure deficit ($VPD_{ant}\times Gness$) and, to a lesser extent, when interacting with antecedent photosynthetically active radiation ($PAR_{ant}\times Gness$). These interactions were consistently negative with VPD and positive with PAR across all treatments, indicating that high VPD and/or low PAR leads to a reduction in predicted R_{eco} relative to the amount of active vegetation present. This likely reflects the effects of these two drivers on photosynthesis. The coupling of R_{eco} and PAR can have important implications for soil respiration (Craine *et al.*,

1999). In addition, high VPD is expected to result in greater stomatal closure (Oren *et al.*, 1999; Damour *et al.*, 2010), reducing GPP and thus root respiration (Yiqi & Zhou, 2010). In forests, maximum leaf area index – like vegetation greenness, a proxy for vegetation productivity – has been found to be a robust predictor to soil respiration across 17 different forest and shrubland sites in Europe and North America (Reichstein *et al.*, 2003). Under elevated CO_2, the interaction between VPD and vegetation greenness is more negative, suggesting an increased sensitivity of stomatal conductance to VPD, which may increase plant water-use efficiency and reduce drawdown of soil water.

Apparent temperature sensitivity (E_o) is an emergent ecosystem property that results from the covariation of many factors with soil temperature, such as soil moisture, substrate availability, and biological activity (Davidson & Janssens, 2006; Sierra, 2012). In this study, E_o was affected by the relative amount of slowly varying (~weekly) plant biomass or phenology, but not by fast timescale drivers (VPD and PAR). In particular, E_o was expected to increase with increasing vegetation greenness (plant biomass) in nonirrigated plots (Table 1), which was particularly pronounced under the combination of elevated CO_2 and warming. This potentially reflects the influence of increased substrates or different substrate types on E_o (Davidson *et al.*, 2006; Hartley & Ineson, 2008), assuming that greenness is a proxy for cumulative substrates and root activity. In contrast to E_o, the main effect of greenness on R_{base} was only significant under irrigation (Table 1), and the statistically significant interaction of greenness and VPD and/or PAR suggests that R_{base} is more strongly coupled to dynamic photosynthesis than plant standing crop. In general, our analysis indicates that aboveground plant activity, whether it be via photosynthesis (for R_{base}) or living biomass (for E_o), is critical for predicting R_{eco}.

Conclusions

We presented a novel analysis of six years of R_{eco} data from a long-term multifactor global change experiment. In summary, our work suggests that R_{eco} predictions can be improved by including the combined effects of antecedent soil moisture, antecedent soil temperature, and aboveground plant activity in future modeling efforts. In fact, the current version of CENTURY, which operates at the daily timescale, illustrates a step toward this goal in that it now includes the effects of moisture conditions prior to rain events and temperature-dependent temperature sensitivity when computing respiration (Del Grosso *et al.*, 2005; Chamberlain *et al.*, 2011). Our results indicate that excluding the effects of antecedent environmental conditions could result in biased (−3.6–17.8%) forecasts of six-year R_{eco} under different global change scenarios. At the landscape to global scale, this suggests that the stimulation of grassland R_{eco} under elevated CO_2 may not be as large as currently predicted (Gilmanov *et al.*, 2010). We recommend that along with past environmental conditions, ecosystem models include aboveground–belowground linkages, both of which appear critical to predicting R_{eco} under current and future climate and CO_2 conditions.

Acknowledgements

This material is based upon work supported by the US Department of Agriculture Agricultural Research Service Climate Change, Soils & Emissions Program, USDA-CSREES Soil Processes Program (#2008-35107-18655), US Department of Energy Office of Science (BER), through the Terrestrial Ecosystem Science program (#DE-SC0006973) and the Western Regional Center of the National Institute for Climatic Change Research, and the National Science Foundation (DEB#1021559). Any opinions, findings, and conclusions or recommendations expressed in this material are those of the author(s) and do not necessarily reflect the views of the National Science Foundation. We thank David Smith for infrastructure maintenance, and Amanda Brennan, Yana Sorokin, Jana Heisler-White, and numerous undergraduate researchers for their help with collecting the data.

References

Adair CE, Reich PB, Trost JJ, Hobbie SE (2011) Elevated CO2 stimulates grassland soil respiration by increasing carbon inputs rather than by enhancing soil moisture. *Global Change Biology*, **17**, 3546–3563.

Arora VK, Boer GJ, Friedlingstein P *et al.* (2013) Carbon-concentration and carbon-climate feedbacks in CMIP5 Earth system models. *Journal of Climate*, **26**, 5289–5314.

Atkin OK, Tjoelker MG (2003) Thermal acclimation and the dynamic response of plant respiration to temperature. *Trends in Plant Science*, **8**, 343–351.

Bachman S, Heisler-White JL, Pendall E, Williams DG, Morgan JA, Newcomb J (2010) Elevated carbon dioxide alters impacts of precipitation pulses on ecosystem photosynthesis and respiration in a semi-arid grassland. *Oecologia*, **162**, 791–802.

Bardgett RD (2011) Plant-soil interactions in a changing world. *F1000 Biology Reports*, **3**, 1–6.

Barron-Gafford GA, Cable JM, Bentley LP, Scott RL, Huxman TE, Jenerette GD, Ogle K (2014) Quantifying the timescales over which exogenous and endogenous conditions affect soil respiration. *New Phytologist*, **202**, 442–454.

Beer C, Reichstein M, Tomelleri E *et al.* (2010) Terrestrial gross carbon dioxide uptake: global distribution and covariation with climate. *Science*, **329**, 834–838.

Bernhardt E, Barber J, Pippen J, Taneva L, Andrews J, Schlesinger W (2006) Long-term effects of free air CO2 enrichment (FACE) on soil respiration. *Biogeochemistry*, **77**, 91–116.

Bond-Lamberty B, Thomson A (2010) Temperature-associated increases in the global soil respiration record. *Nature*, **464**, 579–582.

Booth DT, Cox SE, Berryman RD (2006) Point sampling digital imagery with 'SamplePoint'. *Environmental Monitoring and Assessment*, **123**, 97–108.

Cable JM, Ogle K, Williams DG, Weltzin JF, Huxman TE (2008) Soil texture drives responses of soil respiration to precipitation pulses in the Sonoran Desert: implications for climate change. *Ecosystems*, **11**, 961–979.

Cable JM, Ogle K, Lucas RW *et al.* (2011) The temperature responses of soil respiration in deserts: a seven desert synthesis. *Biogeochemistry*, **103**, 71–90.

Cable JM, Barron-Gafford GA, Ogle K, Pavao-Zuckerman M, Scott RL, Williams DG, Huxman TE (2012) Shrub encroachment alters sensitivity of soil respiration to temperature and moisture. *Journal of Geophysical Research: Biogeosciences*, **2005–2012**, 117.

Cable JM, Ogle K, Barron-Gafford GA *et al.* (2013) Antecedent conditions influence soil respiration differences in shrub and grass patches. *Ecosystems*, **16**, 1230–1247.

Canadell JG, Le Quéré C, Raupach MR *et al.* (2007) Contributions to accelerating atmospheric CO2 growth from economic activity, carbon intensity, and efficiency of natural sinks. *Proceedings of the National Academy of Sciences*, **104**, 18866–18870.

Carbone MS, Winston GC, Trumbore SE (2008) Soil respiration in perennial grass and shrub ecosystems: linking environmental controls with plant and microbial sources on seasonal and diel timescales. *Journal of Geophysical Research: Biogeosciences*, **2005–2012**, 113.

Carrillo Y, Pendall E, Dijkstra FA, Morgan JA, Newcomb JM (2011) Response of soil organic matter pools to elevated CO2 and warming in a semi-arid grassland. *Plant and Soil*, **347**, 339–350.

Carrillo Y, Dijkstra FA, Lecain D, Morgan JA, Blumenthal D, Waldron S, Pendall E (2014) Disentangling root responses to climate change in a semiarid grassland. *Oecologia*, **175**, 699–711.

Chamberlain JF, Miller SA, Frederick JR (2011) Using DAYCENT to quantify on-farm GHG emissions and N dynamics of land use conversion to N-managed switchgrass in the Southern US. *Agriculture, Ecosystems and Environment*, **141**, 332–341.

Chou WW, Silver WL, Jackson RD, Thompson AW, Allen-Diaz B (2008) The sensitivity of annual grassland carbon cycling to the quantity and timing of rainfall. *Global Change Biology*, **14**, 1382–1394.

Ciais P, Reichstein M, Viovy N *et al.* (2005) Europe-wide reduction in primary productivity caused by the heat and drought in 2003. *Nature*, **437**, 529–533.

Clark JS (2003) Uncertainty and variability in demography and population growth: a hierarchical approach. *Ecology*, **84**, 1370–1381.

Cox PM, Betts RA, Jones CD, Spall SA, Totterdell IJ (2000) Acceleration of global warming due to carbon-cycle feedbacks in a coupled climate model. *Nature*, **408**, 184–187.

Craine JM, Wedin DA, Chapin Iii FS (1999) Predominance of ecophysiological controls on soil CO2 flux in a Minnesota grassland. *Plant and Soil*, **207**, 77–86.

Cressie N, Calder CA, Clark JS, Hoef JMV, Wikle CK (2009) Accounting for uncertainty in ecological analysis: the strengths and limitations of hierarchical statistical modeling. *Ecological Applications*, **19**, 553–570.

Damour G, Simonneau T, Cochard H, Urban L (2010) An overview of models of stomatal conductance at the leaf level. *Plant, Cell and Environment*, **33**, 1419–1438.

Davidson EA, Janssens IA (2006) Temperature sensitivity of soil carbon decomposition and feedbacks to climate change. *Nature*, **440**, 165–173.

Davidson E, Belk E, Boone RD (1998) Soil water content and temperature as independent or confounded factors controlling soil respiration in a temperate mixed hardwood forest. *Global Change Biology*, **4**, 217–227.

Davidson EA, Janssens IA, Luo Y (2006) On the variability of respiration in terrestrial ecosystems: moving beyond Q10. *Global Change Biology*, **12**, 154–164.

Davidson EA, Samanta S, Caramori SS, Savage K (2012) The Dual Arrhenius and Michaelis-Menten kinetics model for decomposition of soil organic matter at hourly to seasonal time scales. *Global Change Biology*, **18**, 371–384.

Del Grosso S, Mosier A, Parton W, Ojima D (2005) DAYCENT model analysis of past and contemporary soil N_2O and net greenhouse gas flux for major crops in the USA. *Soil and Tillage Research*, **83**, 9–24.

Desai AR, Richardson AD, Moffat AM *et al.* (2008) Cross-site evaluation of eddy covariance GPP and RE decomposition techniques. *Agricultural and Forest Meteorology*, **148**, 821–838.

Dezi S (2011) Modelling the effects of nitrogen deposition and carbon dioxide enrichment on forest carbon balance.

Dieleman WI, Vicca S, Dijkstra FA *et al.* (2012) Simple additive effects are rare: a quantitative review of plant biomass and soil process responses to combined manipulations of CO2 and temperature. *Global Change Biology*, **18**, 2681–2693.

Dijkstra FA, Carrillo Y, Pendall E, Morgan JA (2013) Rhizosphere priming: a nutrient perspective. *Frontiers in Microbiology*, **4**, 1–8.

Drake JE, Gallet-Budynek A, Hofmockel KS *et al.* (2011) Increases in the flux of carbon belowground stimulate nitrogen uptake and sustain the long-term enhancement of forest productivity under elevated CO2. *Ecology Letters*, **14**, 349–357.

Friedlingstein P, Cox P, Betts R *et al.* (2006) Climate-carbon cycle feedback analysis: results from the C4MIP model intercomparison. *Journal of Climate*, **19**, 3337–3353.

Gelfand AE, Ghosh SK (1998) Model choice: a minimum posterior predictive loss approach. *Biometrika*, **85**, 1–11.

Gelman A, Carlin JB, Stern HS, Rubin DB (2003) *Bayesian Data Analysis*. CRC press, London.

Gelman A, Carlin JB, Stern HS, Dunson DB, Vehtari A, Rubin DB (2013) *Bayesian Data Analysis*. CRC press, London.

Gilmanov TG, Aires L, Barcza Z *et al.* (2010) Productivity, respiration, and light-response parameters of world grassland and agroecosystems derived from flux-tower measurements. *Rangeland Ecology and Management*, **63**, 16–39.

Harmon ME, Bond-Lamberty B, Tang J, Vargas R (2011) Heterotrophic respiration in disturbed forests: a review with examples from North America. *Journal of Geophysical Research: Biogeosciences*, **2005–2012**, 116.

Harper CW, Blair JM, Fay PA, Knapp AK, Carlisle JD (2005) Increased rainfall variability and reduced rainfall amount decreases soil CO2 flux in a grassland ecosystem. *Global Change Biology*, **11**, 322–334.

Hartley IP, Ineson P (2008) Substrate quality and the temperature sensitivity of soil organic matter decomposition. *Soil Biology and Biochemistry*, **40**, 1567–1574.

Högberg P, Read DJ (2006) Towards a more plant physiological perspective on soil ecology. *Trends in Ecology and Evolution*, **21**, 548–554.

Högberg P, Nordgren A, Buchmann N *et al.* (2001) Large-scale forest girdling shows that current photosynthesis drives soil respiration. *Nature*, **411**, 789–792.

Hui D, Verburg P, Arnone J, Luo Y (2008) Dynamics and partitioning of whole ecosystem respiration in a controlled grassland ecosystem. In: Abstract of the Ecological Society of America, 3-8 August, 2008. Milwaukee, Wisconsin.

Huxman TE, Snyder KA, Tissue D *et al.* (2004) Precipitation pulses and carbon fluxes in semiarid and arid ecosystems. *Oecologia*, **141**, 254–268.

Jasoni RL, Smith SD, Arnone JA (2005) Net ecosystem CO2 exchange in Mojave Desert shrublands during the eighth year of exposure to elevated CO2. *Global Change Biology*, **11**, 749–756.

Kimball B (2005) Theory and performance of an infrared heater for ecosystem warming. *Global Change Biology*, **11**, 2041–2056.

Lloyd J, Taylor J (1994) On the temperature dependence of soil respiration. *Functional Ecology*, **8**, 315–323.

Lunn D, Spiegelhalter D, Thomas A, Best N (2009) The BUGS project: evolution, critique and future directions. *Statistics in Medicine*, **28**, 3049–3067.

Luo Y (2007) Terrestrial carbon-cycle feedback to climate warming. *Annual Review of Ecology Evolution, and Systematics*, **38**, 683–712.

Luo Y, Wan S, Hui D, Wallace LL (2001) Acclimatization of soil respiration to warming in a tall grass prairie. *Nature*, **413**, 622–625.

Luo Y, Gerten D, Le Maire G *et al.* (2008) Modeled interactive effects of precipitation, temperature, and [CO2] on ecosystem carbon and water dynamics in different climatic zones. *Global Change Biology*, **14**, 1986–1999.

Miglietta F, Hoosbeek M, Foot J *et al.* (2001) Spatial and temporal performance of the MiniFACE (Free Air CO2 Enrichment) system on bog ecosystems in northern and central Europe. *Environmental Monitoring and Assessment*, **66**, 107–127.

Moldrup P, Olesen T, Yoshikawa S, Komatsu T, Rolston DE (2004) Three-porosity model for predicting the gas diffusion coefficient in undisturbed soil. *Soil Science Society of America Journal*, **68**, 750–759.

Morgan JA, Lecain DR, Pendall E *et al.* (2011) C4 grasses prosper as carbon dioxide eliminates desiccation in warmed semi-arid grassland. *Nature*, **476**, 202–205.

Nie M, Pendall E, Bell C, Gasch CK, Raut S, Tamang S, Wallenstein MD (2013) Positive climate feedbacks of soil microbial communities in a semi-arid grassland. *Ecology Letters*, **16**, 234–241.

Nippert JB, Knapp AK, Briggs JM (2006) Intra-annual rainfall variability and grassland productivity: can the past predict the future? *Plant Ecology*, **184**, 65–74.

Norby RJ, Zak DR (2011) Ecological lessons from free-air CO2 enrichment (FACE) experiments. *Annual Review of Ecology, Evolution, and Systematics*, **42**, 181.

Norby RJ, Hanson PJ, O'neill EG *et al.* (2002) Net primary productivity of a CO2-enriched deciduous forest and the implications for carbon storage. *Ecological Applications*, **12**, 1261–1266.

Ogle K, Barber JJ (2008) Bayesian data—model integration in plant physiological and ecosystem ecology. In: *Progress in Botany*, pp. 281–311. Springer, Berlin, Heidelberg.

Ogle K, Barber JJ, Barron-Gafford GA *et al.* (2015) Quantifying ecological memory in plant and ecosystem processes. *Ecology Letters*, **18**, 221–235.

Oikawa P, Grantz D, Chatterjee A, Eberwein J, Allsman L, Jenerette G (2014) Unifying soil respiration pulses, inhibition, and temperature hysteresis through dynamics of labile soil carbon and O2. *Journal of Geophysical Research: Biogeosciences*, **119**, 521–536.

Oren R, Sperry J, Katul G, Pataki D, Ewers B, Phillips N, Schäfer K (1999) Survey and synthesis of intra-and interspecific variation in stomatal sensitivity to vapour pressure deficit. *Plant, Cell and Environment*, **22**, 1515–1526.

Parslow J, Cressie N, Campbell EP, Jones E, Murray L (2013) Bayesian learning and predictability in a stochastic nonlinear dynamical model. *Ecological Applications*, **23**, 679–698.

Parton WJ, Morgan JA, Wang G, Del Grosso S (2007) Projected ecosystem impact of the prairie heating and CO2 enrichment experiment. *New Phytologist*, **174**, 823–834.

Patrick LD, Ogle K, Bell CW, Zak J, Tissue D (2009) Physiological responses of two contrasting desert plant species to precipitation variability are differentially regulated by soil moisture and nitrogen dynamics. *Global Change Biology*, **15**, 1214–1229.

Pendall E, Leavitt SW, Brooks T *et al*. (2001) Elevated CO2 stimulates soil respiration in a FACE wheat field. *Basic and Applied Ecology*, **2**, 193–201.

Pendall E, Del GS, King JY, Lecain DR, Milchunas DG (2003) Elevated atmospheric CO2 effects and soil water feedbacks on soil respiration components in a Colorado grassland. *Global Biogeochemical Cycles*, **17**, 1046.

Pendall E, Bridgham S, Hanson PJ *et al*. (2004) Below-ground process responses to elevated CO2 and temperature: a discussion of observations, measurement methods, and models. *New Phytologist*, **162**, 311–322.

Pendall E, Heisler-White JL, Williams DG, Dijkstra FA, Carrillo Y, Morgan JA, Lecain DR (2013) Warming reduces carbon losses from grassland exposed to elevated atmospheric carbon dioxide. *PLoS ONE*, **8**, e71921.

Piao S, Ciais P, Friedlingstein P *et al*. (2008) Net carbon dioxide losses of northern ecosystems in response to autumn warming. *Nature*, **451**, 49–52.

Polley HW, Briske DD, Morgan JA, Wolter K, Bailey DW, Brown JR (2013) Climate Change and North American Rangelands: trends, Projections, and Implications. *Rangeland Ecology and Management*, **66**, 493–511.

Reichstein M, Rey A, Freibauer A *et al*. (2003) Modeling temporal and large-scale spatial variability of soil respiration from soil water availability, temperature and vegetation productivity indices. *Global Biogeochemical Cycles*, **17**, 1–15.

Roy J, Mooney HA, Saugier B (2001) *Terrestrial Global Productivity*. Academic Press, San Diego, CA.

Rustad L, Campbell J, Marion G *et al*. (2001) A meta-analysis of the response of soil respiration, net nitrogen mineralization, and aboveground plant growth to experimental ecosystem warming. *Oecologia*, **126**, 543–562.

Schwinning S, Sala OE, Loik ME, Ehleringer JR (2004) Thresholds, memory, and seasonality: understanding pulse dynamics in arid/semi-arid ecosystems. *Oecologia*, **141**, 191–193.

Sierra CA (2012) Temperature sensitivity of organic matter decomposition in the Arrhenius equation: some theoretical considerations. *Biogeochemistry*, **108**, 101–115.

Skopp J, Jawson M, Doran J (1990) Steady-state aerobic microbial activity as a function of soil water content. *Soil Science Society of America Journal*, **54**, 1619–1625.

Sponseller RA (2007) Precipitation pulses and soil CO2 flux in a Sonoran Desert ecosystem. *Global Change Biology*, **13**, 426–436.

Thomas AD, Hoon SR, Linton PE (2008) Carbon dioxide fluxes from cyanobacteria crusted soils in the Kalahari. *Applied Soil Ecology*, **39**, 254–263.

Tucker CL, Bell J, Pendall E, Ogle K (2013) Does declining carbon-use efficiency explain thermal acclimation of soil respiration with warming? *Global Change Biology*, **19**, 252–263.

Vargas R, Carbone MS, Reichstein M, Baldocchi DD (2011) Frontiers and challenges in soil respiration research: from measurements to model-data integration. *Biogeochemistry*, **102**, 1–13.

Wan S, Norby RJ, Ledford J, Weltzin JF (2007) Responses of soil respiration to elevated CO2, air warming, and changing soil water availability in a model old-field grassland. *Global Change Biology*, **13**, 2411–2424.

Williams M, Schwarz PA, Law BE, Irvine J, Kurpius MR (2005) An improved analysis of forest carbon dynamics using data assimilation. *Global Change Biology*, **11**, 89–105.

Xiao C-W, Yuste JC, Janssens I *et al*. (2003) Above-and belowground biomass and net primary production in a 73-year-old Scots pine forest. *Tree Physiology*, **23**, 505–516.

Xu L, Baldocchi DD, Tang J (2004) How soil moisture, rain pulses, and growth alter the response of ecosystem respiration to temperature. *Global Biogeochemical Cycles*, **18**, 1–10.

Yiqi L, Zhou X (2010) *Soil Respiration and the Environment*. Academic press, Burlington, MA.

Zelikova TJ, Pendall E, Williams DG, Hoenigman R, Blumenthal D, Morgan J (accepted) Precipitation controls ecosystem phenology and plant responses to elevated CO2 and warming in a semi-arid grassland. *Ecological Applications*.

Supporting Information

Additional Supporting Information may be found in the online version of this article:

Appendix S1 Description of the (a) gap-filling methods employed for the soil water content (SWC), soil temperature (SoilT), photosynthetically active radiation (PAR), air temperature (AirT) and relative humidity (RH) data; (b) linear interpolation of vegetation greenness data.
Appendix S2 Assessment of model performance.
Figures S1(a–e) Time series of the predicted log(R_{eco}) for 2007, 2008, 2010, 2011 and 2012.
Figure S2 Posterior means and 95% central credible intervals for the antecedent weight parameters.
Figure S3 Correlation between annual R_{eco} and precipitation.
Table S1 Posterior means (standard deviations) for parameters in the R_{eco} mean model (Eqn 2); α_0-α_8 and β_0-β_7 belong to the temperature sensitivity (E_o) and log base rate (log(R_{base})) functions respectively (Eqns 3 and 4)
Table S2 Bayesian *P*-values for each of the 15 pairs of treatment differences for each parameter listed in Table S2a
Table S3 Percentage of data present for the environmental datasets (SWC, SoilT) micrometeorological datasets (PAR, RH, AirT) and the greenness dataset